AoI-optimal Scheduling for Arbitrary K-channel Update-Through-Queue Systems

Won Jun Lee and Chih-Chun Wang
School of ECE, Purdue; Email: {lee4108,chihw}@purdue.edu

***Abstract*—This work generalizes the Age-of-Information (AoI) minimization problem of *update-through-queue* systems such that in addition to deciding the *waiting time*, the sender also chooses over which "channel" each update packet will be served. Different channels have different costs, delays, and quality characteristics that reflect the scheduler's selections of routing, communications, and update modes. Instead of considering only two channels with restricted parameters as in the existing works, this work studies the general K-channel problem with arbitrary parameters. The results show that *both the optimal waiting time and the optimal channel-selection policies admit an elegant water-filling structure*, and can be efficiently computed by the proposed low-complexity fixed-point-based numerical method.**

I. Introduction

Modern networks have ushered in numerous practical applications that require up-to-date data. To reduce data staleness, a source may transmit information to a destination as frequently as possible. At the same time, sending too many packets could congest the network and lead to outdated data. The need to holistically consider data staleness and network dynamics has led to a new performance metric, *Age-of-Information* (AoI), that directly measures data freshness at the destination [1]–[5]. One canonical model of AoI minimization problems is the *update-through-queue* system [6]–[12], where a source sends update packets to a destination through a queue (see our discussion in Sec. II.) With instantaneous delivery acknowledgment, the scheduler varies the *waiting time* to minimize the average AoI. Important variants of this setting include remote sampling [5], [10], distribution oblivious optimal adaptive solutions [13]–[16], delayed feedback [1], [9]–[11], [17], [18], and energy/cost reduction [11], [19].

This work generalizes the update-through-queue model in the following way. In addition to deciding the *waiting time*, the sender also chooses *over which "channel" each update packet will be served.* Different channels have different costs, delays, and quality characteristics that reflect the scheduler's routing, communications, and update modes selections. For example, in Fig. 1 a scheduler has four possible options to send updates: fetching the update from a cloud server through multi-hop Wi-Fi/5G, or from an edge server through single-hop Wi-Fi/5G. Updates from the edge server may be less fresh but are faster and cheaper, whereas updates from the cloud are the freshest but incur longer delays and higher costs. For example, a scheduler in Fig. 1 has four possible choices for sending each update packet. It can fetch the update from a cloud server through multi-hop Wi-Fi or 5G connections. Or it can send the update from an edge server through single-hop Wi-Fi or 5G. An update from the edge server may be slightly outdated (lower quality) but enjoy shorter delay (being closer to the User Equipment (UE)) and cost less, while an update directly from the cloud server will be the freshest (the most accurate) but has a longer delay and higher computational cost. These four choices can be modeled as an abstract "channel" to transmit the update packets. The question to answer is: in terms of data freshness (minimizing AoI), how to dynamically schedule the four "channels" in this system.

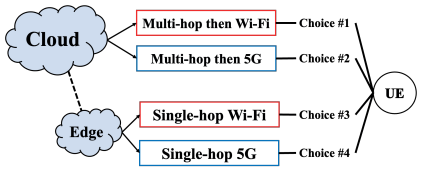

Figure 1. Cloud vs Edge, and Wi-Fi vs 5G

Let's consider an analogy involving package delivery to simplify the understanding of our K-channel AoI minimization system. Picture an online vendor operating both its web shop and an Amazon storefront. This vendor regularly ships products from its factory to Amazon. Now, imagine a customer who always desires the freshest product from this vendor. The vendor faces four main shipping options: 1) Directly sending the package through a courier service like FedEx or UPS; 2) Mailing the package via a postal service such as USPS; 3) Shipping the product through Amazon using its express delivery service; 4) Sending the product via Amazon without opting for express delivery (where Amazon might use a courier service). The customer places a new order immediately upon receiving a package. The vendor aims to determine the optimal shipping time to ensure product freshness while considering the associated costs. Shipping through Amazon introduces some staleness to the product but is faster, albeit at a price. Direct shipping preserves freshness and is more cost-effective but incurs a longer delivery time. While immediate shipping might appear ideal, we know the value of strategic waiting, as discussed in Sun et al. (2017) [8]. Therefore, the vendor must make two critical decisions: choosing the shipping channel and determining the optimal waiting period. This paper explores the vendor's strategy (optimal policy) to maintain the product's highest possible freshness (or information currency).

Existing works in this important multichannel setting are

still nascent.[1] For example, [23] discovered a threshold-like aging control policy when one can choose between Wi-Fi and 5G. Similarly, [24] minimized the AoI while considering sub-6GHz and mmWave channels jointly. In both works, there are exactly two channels. Both are of straightforward channel models: [23] modeled Wi-Fi as a low-cost, random-on/off channel, and 5G as a high-cost, always-on channel; [24] modeled mmWave as a Gilbert-Elliot channel and sub-6GHz as a *deterministic-delay* channel. Motivated by modern networks generally supporting many transmission options with diverse delay and cost characteristics, e.g., Wi-Fi, 5G, Zigbee, Bluetooth, this work considers general K-channel systems with arbitrary delay distributions, cost and quality characteristics. Our main contributions are:

(i) We prove that in a multichannel system, the optimal waiting time follows the same water-filling structure [3], [8] as in the single-channel case.

(ii) We prove that the optimal channel selection policy is *in the reverse order of the expected delays*. That is, the optimal scheduler would choose a channel with longer *expected delay* if the current AoI is small and switch to a channel with shorter expected delay if the current AoI is large. "When to switch" depends on the cost differences between competing channels, formally characterized in Sec. III.

(iii) We further strengthen (ii) by proving that *the optimal channel selection policy also admits a water-filling structure.*

(iv) Leveraging on the findings in (i) and in (iii), we design a low-complexity fixed-point-based method that efficiently computes the optimal scheduler for arbitrary K-channel systems.

II. Problem Formulation

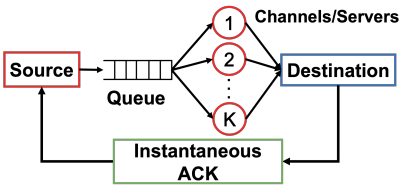

Figure 2. The K-channel Update-Through-Queue System

We model the multi-choice information update scenario in Sec. I as a single-source/single-destination update system with different *channel choices*. Each (abstract) channel represents one combination of the *origin* of the update packet, e.g., cloud vs. edge, and the communication mode, e.g., 5G vs. Wi-Fi. It is single-source since the "source" represents the central scheduler, not the different possible origins of the packets. It is single-destination since it represents a (single) user that consumes all the updated information. The detailed analytical model is formally defined below.

Consider the system in Fig. 2 and assume *continuous* time axis. At any time $t \in \mathbb{R}^+$, the source can inject an information update packet P_i to a First-In-First-Out (FIFO) queue. In addition to deciding when to inject an update packet, i.e., deciding the *waiting time*, the scheduler must also specify which server will be used to service the packet. To avoid confusion with the terms "cloud and edge servers" in our motivating scenario, we change the term "server" to "channel" when discussing our model. That is, all packets share a common FIFO queue, and each packet has embedded channel-index k in its header and will be served by CH_k when it is its turn. The choice of channels is made separately for each packet P_i.

When the service of an update packet is complete (i.e., upon delivery), the destination will feedback an instantaneous ACK. We aim to characterize the jointly optimal waiting time and channel selection policy that minimizes the AoI.

To provide further details, we assume there are K channels. Each channel CH_k, $k \in \mathcal{C} \triangleq \{1, 2, \cdots, K\}$ is characterized by the following three attributes that are known globally:

• **Delay distribution:** The service time (delay) of each CH_k is i.i.d. with bounded support. We denote the (marginal) distribution by $P(Y^{[k]})$.

We assume the channels are indexed by the ascending order of the expected delays. Namely,

$$\mathbb{E}(Y^{[1]}) \leq \mathbb{E}(Y^{[2]}) \leq \ldots \leq \mathbb{E}(Y^{[K]}) < \infty. \tag{1}$$

• **Update quality degradation:** Recall that each "channel" represents a combination of (a) the origin of the update packets and (b) the medium of communications, see Fig. 1. For each CH_k, we use $\mathsf{Lag}_k \geq 0$ to represent the *quality degradation* of the update packets due to (a). The larger the Lag_k, the more outdated the update packet is, the worse the quality. For example, a channel that represents fetching the update packet from a cloud server may have $\mathsf{Lag} = 0$ while a channel that represents fetching the update from an edge server may have $\mathsf{Lag} = 5$. The latter signifies that the data quality at the edge server is roughly *5-temporal-units-more-outdated* than the data at the cloud server. We assume such a conversion from the update quality to the equivalent time-lag Lag_k is possible and known to the scheduler.

We assume the values of Lag_k are given and known. Also, see the discussion around Eq. (2) for the intuition of Lag_k.

• **Transmission cost:** Since our "channels" also represent (b) the medium of communications, we use Cst_k to denote the (monetary or energy) cost of sending one packet over CH_k.

Define the send time and arrival time of the i-th packet P_i by S_i and A_i, respectively. At any time t, define $i^*(t) = \arg\max\{i : A_i \leq t\}$ as the index of the most recently delivered packet. The AoI $\Delta(t)$ is then defined by

$$\Delta(t) \triangleq t - S_{i^*(t)} + \mathsf{Lag}_{k(i^*(t))} \tag{2}$$

where $k(i^*(t))$ is the channel that delivered packet $P_{i^*(t)}$.

The best way to interpret (2) is to first assume $\mathsf{Lag}_k = 0, \forall k$. Eq. (2) is then equivalent to the traditional definition of AoI in [25], [26]. Recall that if we fetch the update from an edge server, its quality would be worse than if fetching it directly from a cloud server. As a result, if the latest packet $P_{i^*(t)}$ is

[1]This paper focuses exclusively on the single-source system. For the multiple-source systems [20]–[22], the goal is to balance the AoI across coexisting source-destination pairs, which is very different from our goal of minimizing AoI of a single (and only) source-destination pair.

from $\mathsf{CH}_{k(i^*(t))}$, we "penalize" the *effective AoI* $\Delta(t)$ by the quality degradation term $\mathsf{Lag}_{k(i^*(t))}$.

The scheduler at the source must decide the send time S_i of each update, and over which channel $k(i)$ it will be served, with the goal of solving the following minimization problem:

$$\beta^* \triangleq \inf_{\text{all policies}} \limsup_{T\to\infty} \frac{\mathbb{E}\left\{\int_0^T \Delta(t)\,dt + \sum_{i=1}^{i^*(T)} \mathsf{Cst}_{k(i)}\right\}}{T} \tag{3}$$

Limitations of our model: While our single-queue, multi-channel model is unambiguously defined, it does not fully capture the motivating scenario in Sec. I. For example, as will be shown later, the optimal policy under our model will never send a new packet before the older packet is delivered. (Existing works [23], [24] do not allow for parallel transmission either.) However, in the scenario of Fig. 1, the UE may request parallel updates simultaneously to improve the timeliness further. Further generalization of our model is needed to fully reflect the motivating scenario of Fig. 1.

III. Main Results

A. Conversion to an ACPS-Semi-MDP Problem

We first show that (3) is a semi-Markov Decision Process (semi-MDP) with continuous state $s \in \mathbb{R}^+$, where s represents the AoI $\Delta(t)$ when deciding at time t.

Since we use *generate-at-will* model [8], and because it is AoI-suboptimal [8] to let any update packet wait in the queue, an optimal scheduler only needs to make the decision of the send time S_i at time $t = A_{i-1}$, i.e., at the instant when the previous packet was delivered.

The action space $\mathcal{A}$ for any state s is defined by

$$\mathcal{A} \triangleq \{\,(k,w) : k \in \mathcal{C}, w \in \mathbb{R}^+\,\} \tag{4}$$

where w is the *waiting time*, i.e., the send time being $S_i = A_{i-1} + w$; and k is the channel that serves packet P_i.

If action (k,w) is chosen for state s at time $t = A_{i-1}$, then the state transition probability becomes[2]

$$p_{s\tilde{s}}^{(k,w)} \triangleq P\left(Y^{[k]} + \mathsf{Lag}_k = \tilde{s}\right) \tag{5}$$

Namely, at the delivery time $t = A_i = S_i + Y_i^{[k]}$, we have the new state $\tilde{s} = \Delta(A_i) = Y_i^{[k]} + \mathsf{Lag}_k$ by (2).

Our problem is a semi-MDP instead of a regular MDP because the *sojourn time* from state s to the new state $\tilde{s}$ under action (k,w) is a random variable characterized by [27]

$$\tau(k,w) \triangleq A_i - A_{i-1} = w + Y_i^{[k]}. \tag{6}$$

For convenience, we define the expectation of $\tau(k,w)$ by

$$\overline{\tau}(k,w) \triangleq \mathbb{E}\{\tau(k,w)\} = w + \mathbb{E}(Y^{[k]}) \tag{7}$$

[2]Because we consider continuous time axis, a more accurate but more burdensome description should be $p_{s\to d\tilde{s}}^{(k,w)} = P\left(Y^{[k]} + \mathsf{Lag}_k \in d\tilde{s}\right)$. For notational simplicity, we deliberately avoid using $d\tilde{s}$ in our formulation.

We now quantify the AoI+cost per action. Specifically, the cost of action (k,w) at state s is

$$c(s,k,w) \triangleq 0.5\left(\left(s + w + Y^{[k]}\right)^2 - s^2\right) + \mathsf{Cst}_k \tag{8}$$

where the first term is the AoI area due to sending P_i, see Fig. 3, and the last term Cst_k is the cost of using CH_k. Taking the expectation of $c(s,k,w)$ in (8) and simplifying it, we have

$$\overline{c}(s,k,w) \triangleq s\cdot\left(\mathbb{E}(Y^{[k]}) + w\right) + 0.5\cdot\mathbb{E}\left\{(Y^{[k]} + w)^2\right\} + \mathsf{Cst}_k \tag{9}$$

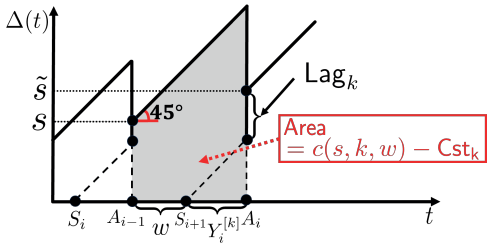

Figure 3. Evolution of The AoI

Using the above semi-MDP definitions, a scheduling policy $\pi : \mathbb{R}^+ \mapsto \mathcal{C}\times\mathbb{R}^+$, which maps the state value s to the corresponding channel and waiting-time choices (k,w), will have its average total cost per unit time being[3]

$$J^\pi = \lim_{I\to\infty} \frac{\mathbb{E}\left\{\sum_{i=0}^{I-1} \overline{c}\left(\Delta(A_i), \pi(\Delta(A_i))\right)\right\}}{\mathbb{E}\left\{\sum_{i=0}^{I-1} \overline{\tau}\left(\pi(\Delta(A_i))\right)\right\}} \tag{10}$$

The optimal π^* that minimizes J^π satisfies the following Bellman equation for all $s \in \mathbb{R}^+$ [27]):

$$h(s) = \min_{\substack{k\in\mathcal{C}\\ w\in\mathbb{R}^+}} \left\{\overline{c}(s,k,w) - \overline{\tau}(k,w)\cdot\beta^* + \int_{\tilde{s}=0}^{\infty} p_{s\tilde{s}}^{(k,w)} h(\tilde{s})\,d\tilde{s}\right\} \tag{11}$$

where $\overline{\tau}(k,w)\cdot\beta^*$ is the adjustment term when computing the average cost per unit time.

Proposition 1. The optimal value β^*, defined in (3), can be found by solving the β^* satisfying the Bellman equation (11).

B. Waiting Time versus Channel Selection

In this subsection, we further simplify (11). Define the expression in (11) without the min operation by

$$Q_k(s,w,\beta^*) \triangleq \overline{c}(s,k,w) - \overline{\tau}(k,w)\beta^* + \int_{\tilde{s}=0}^{\infty} p_{s\tilde{s}}^{(k,w)} h(\tilde{s})\,d\tilde{s}$$

By plugging in the expressions of $\overline{c}(s,k,w)$, $\overline{\tau}(k,w)$ and $p_{s\tilde{s}}^{(k,w)}$ in (9), (7), and (5), respectively, we can easily simplify $Q_k(s,w,\beta^*)$ as follows:

$$Q_k(s,w,\beta^*) = Q_k^\circ(s,w,\beta^*) - \frac{(s-\beta^*)^2}{2} \tag{12}$$

[3]Without loss of generality, we assume the initial state $s_0 = \Delta(0) = 0$.

where

$$Q_k^\circ(s,w,\beta^*) \triangleq \frac{\big((s+w)-\big(\beta^*-\ \mathbb{E}(Y^{[k]})\big)\big)^2}{2}+\mathcal{H}_k \quad (13)$$

and we use the *variance* of $Y^{[k]}$ to define

$$\mathcal{H}_k \triangleq \frac{\mathsf{var}(Y^{[k]})}{2}+\mathbb{E}\{h(\mathsf{Lag}_k+Y^{[k]})\}+\mathsf{Cst}_k. \quad (14)$$

We then notice that the term $\frac{(s-\beta^*)^2}{2}$ in (12) does not depend on the policy choice (k,w). Therefore, from the perspective of characterizing the optimal policy, we can focus on minimizing $Q_k^\circ(s,w,\beta^*)$ instead of $Q_k(s,w,\beta^*)$. Note that we can temporarily ignore the $\frac{(s-\beta^*)^2}{2}$ term in (12), since it does not depend on the policy choice w.

Proposition 2. Given any fixed k, the waiting time w^* that minimizes $Q_k^\circ(s,w,\beta^*)$ follows a water-filling structure:

$$w^* = \max(\beta^*-\mathbb{E}(Y^{[k]})-s,0) \quad (15)$$

$$= \max\{w\geq 0: w+s+\mathbb{E}(Y^{[k]})\geq\beta^*\}. \quad (16)$$

Furthermore, if we plot $\min_{w\geq 0} Q_k^\circ(s,w,\beta^*)$ as a function of s, see Fig. 4, it consists of two halves: the left-hand side of the vertex ($s=\beta^*-\mathbb{E}(Y^{[k]})$) is a flat line while the right-hand side being identical to the quadratic curve $Q_k^\circ(s,0,\beta^*)$.

Namely, the optimization over $w\geq 0$ essentially "bends" the left-hand side of the quadratic curve $Q_k^\circ(s,0,\beta^*)$ downwards to a flat line. See [28] for additional details.

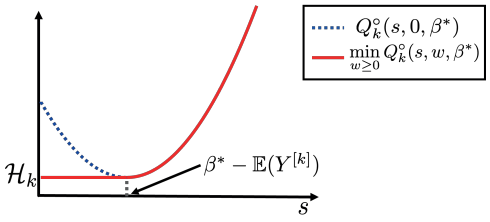

Figure 4. $Q_k^\circ(s,0,\beta^*)$ versus $\min_{w\geq 0} Q_k^\circ(s,w,\beta^*)$

Because the optimal waiting time in (15)–(16) for our multichannel setting is of an identical form as the single-channel case [3], [29], [30], it implies that ***an overall optimal policy can be done sequentially: Firstly, we choose the optimal*** CH_k***, and then we choose the optimal waiting time of*** P_i ***using*** (16) ***as if we are in a single-channel scenario.***

We now describe the optimal channel selection for the $K=2$ case. Specifically, Fig. 5 plots two curves defined as follows:

$$Q_k^\star(s,\beta^*) \triangleq \min_{w\geq 0} Q_k^\circ(s,w,\beta^*), \quad \forall k\in\{1,2\} \quad (17)$$

Following the discussion right after Eq. (14), the optimal policy will solve $\min_{(k,w)} Q_k^\circ(s,w,\beta^*) = \min_k Q_k^\star(s,\beta^*)$, which can be solved by analyzing the relative positions between $Q_1^\star(s,\beta^*)$ and $Q_2^\star(s,\beta^*)$. Specifically, there is a threshold θ^*, see Fig. 5, such that we choose $k=2$ if $s<\theta^*$ and choose $k=1$ if $s\geq\theta^*$. The θ^* is the intersecting point of the two curves $Q_1^\star(s,\beta^*)$ and $Q_2^\star(s,\beta^*)$, assuming

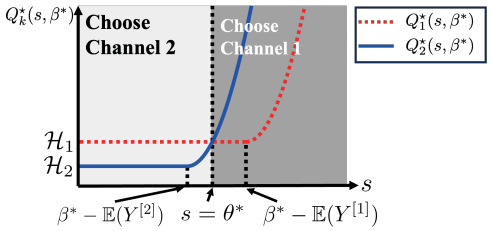

Figure 5. Optimal channel selection for the $K=2$ channel system

we know the values of $\beta^*, \mathbb{E}(Y^{[k]})$, and $\mathcal{H}_k$. The θ^* value can be easily found by calculating the intersecting point of two curves $Q_1^\star(s,\beta^*)$ and $Q_2^\star(s,\beta^*)$, assuming we know the values of $\beta^*, \mathbb{E}(Y^{[k]})$, and $\mathcal{H}_k$.

We now generalize the above discussion for arbitrary K:

Proposition 3. The optimal channel selection policy is of the following *water-filling* structure. Each CH_k has a *water-level value* γ_k where $\gamma_1\leq\gamma_2\leq\cdots\leq\gamma_K=\infty$ and each value can be positive or negative. The corresponding channel selection rule under a given state s is described by

$$k^*(s) = \min\{k\in\{1,\cdots,K\}: \gamma_k+s\geq\beta^*\}. \quad (18)$$

The proof is derived by jointly comparing the relative positions of all K curves $Q_k^\star(s,\beta^*)$. We thus omit the details.

A few remarks are in order. Firstly, (18) has the same water-filling structure as in (16). Secondly, the selection rule (18) is *monotonic*, i.e., when s is small, we would select the channel with a larger k (since γ_k is non-decreasing), and vice versa Finally, Proposition 3 implies implicitly that if $\gamma_k=\gamma_{k+1}$, then, by definition, the selection rule (18) will *never* select CH_{k+1}. It means that CH_{k+1} is "dominated" by other channels, a phenomenon frequently encountered in our simulations.

Note that given β^* and $\mathbb{E}(Y^{[k]})$, the optimal $w^*(s)$ is fully described by (16), but $k^*(s)$ in (18) still depends on the values of γ_k. We now describe how to compute γ_k assuming we know the values of β^* and $\mathcal{H}_k$, the latter of which can easily be computed via (14) if we know the function $h(s)$ and the distribution of $Y^{[k]}$. The optimal channel selection policy is complete once we have computed γ_k, the optimal channel selection policy is complete.

Lemma 1. Consider any given two channels CH_i and CH_j. We then have two cases.

Case 1: $\mathbb{E}(Y^{[i]})=\mathbb{E}(Y^{[j]})$. If $\mathcal{H}_i=\mathcal{H}_j$, then the two curves $Q_i^\star(s,\beta^*)$ and $Q_j^\star(s,\beta^*)$ are identical, see (13). If $\mathcal{H}_i\neq\mathcal{H}_j$, then $Q_i^\star(s,\beta^*)$ and $Q_j^\star(s,\beta^*)$ are *parallel*, and do not intersect.

Case 2: $\mathbb{E}(Y^{[i]})<\mathbb{E}(Y^{[j]})$. We have three subcases. **Case 2.1:** If $\mathcal{H}_i<\mathcal{H}_j$, then $Q_i^\star(s,\beta^*)$ and $Q_j^\star(s,\beta^*)$ have no intersecting point; **Case 2.2:** If $\mathcal{H}_i=\mathcal{H}_j$, then the two curves fully overlap for the range of $s\leq\beta^*-\mathbb{E}(Y^{[j]})$; **Case 2.3:** If $\mathcal{H}_i>\mathcal{H}_j$, then the two curves have exactly one intersecting

point at $s = \theta_{i,j}$ regardless of the β^* value. The intersecting $s = \theta_{i,j}$ value can be expressed by

$$\theta_{i,j} = \beta^* - f_\gamma\left(\mathbb{E}(Y^{[i]}), \mathbb{E}(Y^{[j]}), \mathcal{H}_i - \mathcal{H}_j\right) \quad (19)$$

and the description of $f_\gamma(\cdot,\cdot,\cdot)$ is provided in Appendix C.

Using Lemma 1, Algorithm 1 computes the values of $\gamma_k, \forall k \in \mathcal{C}$. We omit the proof due to space constraints.

Algorithm 1 Computing the water-level values γ_k

Require: $\mathbb{E}(Y^{[k]})$,$\mathcal{H}_k$, $\forall k \in \mathcal{C}$, and the $f_\gamma(\cdot,\cdot,\cdot)$ in (19).

1: $\mathcal{P}$ is a set of *ordered pairs*; initialize $\mathcal{P} \leftarrow \emptyset$.
2: **for** all $i, j \in \mathcal{C}$ and $i < j$ **do**
3: Consider the two curves $Q_i^\star(s, \beta^*)$ and $Q_j^\star(s, \beta^*)$.
4: **if** they have exactly one intersecting point **then**

$$\tilde{\gamma}_{i,j} \leftarrow f_\gamma\Big(\mathbb{E}(Y^{[i]}), \mathbb{E}(Y^{[j]}), \mathcal{H}_i - \mathcal{H}_j\Big); \quad \mathcal{P} \leftarrow \mathcal{P} \cup \{(i,j)\}$$

5: **end if**
6: **end for**
7: $j_0 \leftarrow \arg\min_{k \in \mathcal{C}} \mathcal{H}_k$.
8: $\gamma_k \leftarrow -\infty, \forall k \in (0, j_0)$; and $\gamma_k \leftarrow \infty, \forall k \in [j_0, K]$.
9: **while** $j_0 \geq 2$ **do**
10: $i_0 \leftarrow \arg\max_{(i,j_0) \in \mathcal{P}} \tilde{\gamma}_{i,j_0}$
11: **if** $i_0 \geq 1$ **then**
12: $\gamma_k \leftarrow \tilde{\gamma}_{i_0,j_0}, \forall k \in [i_0, j_0)$.
13: **end if**
14: $j_0 \leftarrow i_0$.
15: **end while**

Note 1: If there is a tie in Line 7, choose the smallest such j_0. If there is a tie in Line 10, choose the smallest such i_0.
Note 2: In Line 10, if no $(i, j_0) \in \mathcal{P}$, then $i_0 \leftarrow -\infty$.

C. Numerical Computation via Fixed-Point Iteration

This subsection discusses how to compute the optimal β^* and the value function $h(s)$, which can then be used to compute $w^*(s)$ using (15), compute $\mathcal{H}_k$ using (14), compute γ_k using Algorithm 1, and compute $k^*(s)$ using (18). Our method is very efficient since it utilizes the optimal water-filling structures during the fixed-point iteration computation.

Lemma 2. When solving the Bellman equation (11), we only need to consider a bounded range of $s \in [0, y_{\max} + \max_k \mathsf{Lag}_k]$ instead of the unbounded range of $s \in \mathbb{R}^+$.

The proof is provided in [28]. By Lemma 2, we quantize the interval $[0, y_{\max} + \max_k \mathsf{Lag}_k]$ with N grid points

$$\mathcal{S}_N \triangleq \left\{ n \cdot \frac{y_{\max} + \max_k \mathsf{Lag}_k}{N} : n \in \{0, 1, \cdots N-1\} \right\} \quad (20)$$

for some sufficiently large N. Namely, we only solve the β^* and the $h(s)$ values for a finite number of $s \in \mathcal{S}_N$. The functions $\overline{c}(s,k,w)$ and $\overline{\tau}(k,w)$ do not change during quantization. They are still specified by (9) and (7), respectively. However, $p_{s\tilde{s}}^{(k,w)}$ in (5) will change slightly since the next state $\tilde{s}$ is also quantized to grid points in $\mathcal{S}_N$. We thus need to reassign the probability from the continuous pdf $P(Y^{[k]} \in dy)$ to their discrete pmf counterpart. Such a reassignment is standard when quantizing any continuous random variable.

We then solve the quantized Bellman equation (11) over $s \in \mathcal{S}_N$ in an iterative fashion: We initialize $\beta^{(0)} = 0$ and $h^{(0)}(s) = 0, \forall s \in \mathcal{S}_N$. Then, for $l \geq 1$, we do the following.

Step 1: Use $h^{(l-1)}(s)$ to compute $\mathcal{H}_k^{(l-1)}$ using (14) and the (quantized) distribution of $P(Y^{[k]})$.

Step 2: Use $\beta^{(l-1)}$ and $\mathcal{H}_k^{(l-1)}$ to compute the optimal channel selection rule $k^{(l)}(s)$ using (18) and Algorithm 1. Use $\beta^{(l-1)}$ and $\mathbb{E}(Y^{[k]})$ to compute the optimal waiting time $w_k^{(l)}(s)$ for each CH_k. Collectively, $k^{(l)}(s)$ and $w_k^{(l)}(s)$ form a scheduling policy, which we denote as $\pi^{(l)}$.

Step 3: Replace the $\min_{(k,w)}$ operator in (11) by the policy $\pi^{(l)}$. Namely, we have a simple linear equation: $\forall s \in \mathcal{S}_N$.

$$h(s) = \overline{c}(s, k(s), w(s)) - \overline{\tau}(k(s), w(s))\beta + \sum_{\tilde{s} \in \mathcal{S}_N} p_{s\tilde{s}}^{(k(s),w(s))} h(\tilde{s}) \quad (21)$$

where $k(s)$ and $w(s)$ are the action choices under policy $\pi^{(l)}$. We then solve the β and $h(s)$ values that satisfy (21) for all $s \in \mathcal{S}_N$ while hardwiring $h(0) = 0$ when finding the solution. We denote the end results by $\beta^{(l)}$ and $h^{(l)}(s)$, respectively. [4]

Step 4: Repeat Steps 1 to 3 until $\beta^{(l)}$ and $h^{(l)}(s)$ converge.

Lemma 3. Assume a sufficiently large N such that the quantized computation mimics the original continuous-time counterpart. In the above 4-step process, the resulting $\beta^{(l)}$ is a non-increasing function when $l \geq 1$ (excluding $l = 0$), and $\lim_{l \to \infty} \beta^{(l)} = \beta^*$.

IV. Numerical Evaluations

Consider a 4-ch system described in Table I, for which the channel index is sorted in the ascending order of $\mathbb{E}(Y^{[k]})$ as required in Sec. II. The example scenario is related to our discussion of Fig. 1, i.e., an update from the edge server will experience an AoI degradation $\mathsf{Lag} = 5$. We assume 5G and single-hop have shorter delays than Wi-Fi and multi-hop communications. We assign Cst_k in the reverse order of $\mathbb{E}(Y^{[k]})$ to avoid the less interesting cases that one channel is dominated by other channels. Otherwise, the problem will collapse to a simple 1-channel or 2-channel case, making the setting less enjoyable.

Fig. 6(a) tracks the convergence of $\beta^{(l)}$ in our proposed method. In Fig. 6(b), we use a generic Q-function value iteration [31] to solve the semi-MDP in (11). While convergence is guaranteed for both methods, both outputting the same $\beta^* = 18.93$, the Q-value iteration took hundreds of iterations to converge. In contrast, our low-complexity algorithm converged in just a few iterations ($l \approx 4$).

We also compare with some other non-trivial solutions. Specifically, we designed separately a policy that hardwires

[4] Solving the linear equations does not necessarily involve matrix inversion. In our setting, the linear equations contain some *contraction mappings*, and the solution can be found by simple fixed-point iterations that first find the steady-state distribution, then find $\beta^{(l)}$, and finally find $h^{(l)}(s)$.

Table I
SIMULATION CHANNEL PARAMETERS

	Example	Distribution $P(Y^{[k]})$	Lag_i	Cst_i
CH_1	**Edge+5G**	uniform over $\{1,2,4,5\}$ $\mathbb{E}(Y^{[1]})=3$	5	150
CH_2	**Cloud+5G**	uniform over $\{1,4,8,11\}$ $\mathbb{E}(Y^{[2]})=6$	0	100
CH_3	**Edge+Wi-Fi**	uniform over $\{1,7,9,15\}$ $\mathbb{E}(Y^{[3]})=8$	5	50
CH_4	**Cloud+Wi-Fi**	uniform over $\{1,11,13,23\}$ $\mathbb{E}(Y^{[4]})=12$	0	0

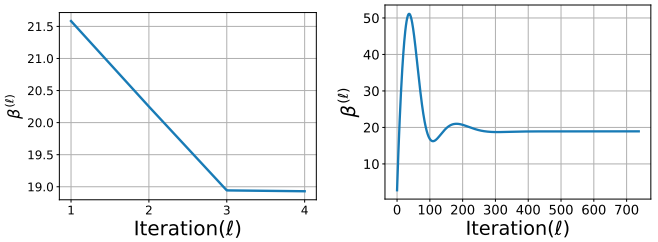

(a) Proposed Iterative Algorithm (b) Q Value Iteration [31]

Figure 6. Convergence behavior of $\beta^{(\ell)}$

$w=0$, i.e., zero-wait, but optimally switches between different CH_k depending on the state $s=\Delta(t)$. We also designed "dumb" deterministic channel selection policies (say always choose CH_k), but with optimal waiting time w^*, [8], [9]. We call them "single-ch$k$ policies". In Figs. 7(a) and 7(b), we multiply the cost Cst_k in Table I of each channel by a common factor $\alpha\in[1,2]$. We then plot the optimal β^* versus different α. Fig. 7(a) reaffirms that varying the waiting time is crucial to achieve β^* since our scheme significantly outperforms ZW-opt, which optimizes only channel selection but not waiting time. The same setup is repeated in Fig. 7(b), but we focus on single-ch$k$ policies this time. By dynamically utilizing the best of the 4 channels for different state s, our optimal scheme consistently outperforms any single-ch$k$ policy. Note that when $\alpha\geq 1.7$, single-ch4 becomes optimal as all other channels become too costly with the new cost $\alpha\mathsf{Cst}_k$. In sum, our algorithm takes full advantage of the heterogeneity of K channels. It employs only the best channel and best waiting time at any given state s, the key to optimal performance.

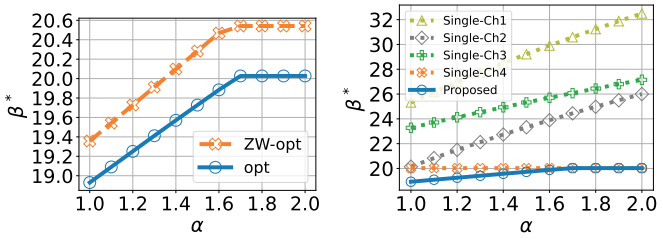

(a) Versus Zero-Wait Policy (b) Versus Single-Channel Policy

Figure 7. Achievable AoI compared to other non-trivial solutions.

V. CONCLUSION

We have studied AoI minimization for heterogeneous K-channel systems and fully characterized the optimal scheduler. New *water-filling* structures of optimal policies and efficient computation methods have been discovered. One potential application is the AoI-optimal scheduling over multiple cloud vs edge transmission choices and 5G vs Wi-Fi, respectively.

ACKNOWLEDGMENT

This work was supported in parts by NSF Grants CNS-2008527, CNS-2107363, and CCF-2309887, as well as by under grant National Spectrum Consortium (NSC) W15QKN-15-9-1004.

REFERENCES

[1] C.-C. Wang, "How useful is delayed feedback in AoI minimization — a study on systems with queues in both forward and backward directions," in *2022 Proc. IEEE Intl. Symp. Inform. Theory (ISIT)*. Espoo, Finland: IEEE, Jun. 2022, pp. 3192–3197. [Online]. Available: https://ieeexplore.ieee.org/document/9834697/

[2] J. Zhang and C.-C. Wang, "On the rate-cost of gaussian linear control systems with random communication delays," in *2018 IEEE Intl. Symp. Inform. Theory (ISIT)*. Vail, CO, USA: IEEE Press, Jun. 2018, p. 2441–2445. [Online]. Available: https://doi.org/10.1109/ISIT.2018.8437916

[3] Y. Sun and B. Cyr, "Sampling for data freshness optimization: Non-linear age functions," *J. Commun. Netw.*, vol. 21, no. 3, pp. 204–219, 2019.

[4] T. Z. Ornee and Y. Sun, "Sampling and remote estimation for the ornstein-uhlenbeck process through queues: Age of information and beyond," *IEEE/ACM Trans. Netw.*, vol. 29, no. 5, pp. 1962–1975, Oct. 2021.

[5] Y. Sun, Y. Polyanskiy, and E. Uysal, "Sampling of the wiener process for remote estimation over a channel with random delay," *IEEE Trans. Inform. Theory*, vol. 66, no. 2, pp. 1118–1135, Feb. 2020. [Online]. Available: https://ieeexplore.ieee.org/document/8812616/

[6] L. Huang and E. H. Modiano, "Optimizing age-of-information in a multi-class queueing system," *2015 IEEE Intl. Symp. Inform. Theory (ISIT)*, pp. 1681–1685, Apr. 2015. [Online]. Available: https://api.semanticscholar.org/CorpusID:5889182

[7] V. Tripathi, R. Talak, and E. H. Modiano, "Age of information for discrete time queues," January 2019, [Online]. Available: https://api.semanticscholar.org/CorpusID:59413906.

[8] Y. Sun, E. Uysal-Biyikoglu, R. D. Yates, C. E. Koksal, and N. B. Shroff, "Update or wait: How to keep your data fresh," *IEEE Trans. Inf. Theory*, vol. 63, no. 11, pp. 7492–7508, Nov. 2017.

[9] C.-H. Tsai and C.-C. Wang, "Age-of-information revisited: Two-way delay and distribution-oblivious online algorithm," in *2020 IEEE Intl. Symp. Inform. Theory (ISIT)*, Los Angeles, CA, USA, 2020, pp. 1782–1787.

[10] ——, "Unifying AoI minimization and remote estimation—optimal sensor/controller coordination with random two-way delay," *IEEE/ACM Trans. Networking*, vol. 30, no. 1, pp. 229–242, Feb. 2022. [Online]. Available: https://ieeexplore.ieee.org/document/9540757/

[11] ——, "Jointly minimizing AoI penalty and network cost among coexisting source-destination pairs," in *2021 IEEE Intl. Symp. Inform. Theory (ISIT)*, Melbourne, Australia, 2021, pp. 3255–3260.

[12] R. D. Yates and S. K. Kaul, "The age of information: Real-time status updating by multiple sources," *IEEE Trans. Inform. Theory*, vol. 65, no. 3, pp. 1807–1827, 2019.

[13] C.-H. Tsai and C.-C. Wang, "Distribution-oblivious online algorithms for age-of-information penalty minimization," *IEEE/ACM Trans. Networking*, vol. 31, no. 4, pp. 1779–1794, Aug. 2023. [Online]. Available: https://ieeexplore.ieee.org/document/10012322/

[14] C. Kam, S. Kompella, and A. Ephremides, "Learning to sample a signal through an unknown system for minimum AoI," in *IEEE INFOCOM 2019 - IEEE Conf. Comput. Commun. Workshops (INFOCOM WKSHPS))*. Paris, France: IEEE, 2019, pp. 177–182. [Online]. Available: https://ieeexplore.ieee.org/document/8845311/

[15] E. U. Atay, I. Kadota, and E. H. Modiano, "Aging bandits: Regret analysis and order-optimal learning algorithm for wireless networks with stochastic arrivals," Dec. 2020. [Online]. Available: https://api.semanticscholar.org/CorpusID:229220264

[16] H. Tang, Y. Chen, J. Sun, J. Wang, and J. Song, "Sending timely status updates through channel with random delay via online learning," in *IEEE INFOCOM 2022 - IEEE Conf. Comput. Commun.* London, United Kingdom: IEEE Press, May. 2022, p. 1819–1827. [Online]. Available: https://doi.org/10.1109/INFOCOM48880.2022.9796970

[17] J. Pan, A. M. Bedewy, Y. Sun, and N. B. Shroff, "Optimal sampling for data freshness: Unreliable transmissions with random two-way delay," *IEEE/ACM Trans. Networking*, vol. 31, no. 1, pp. 408–420, Feb. 2023. [Online]. Available: https://ieeexplore.ieee.org/document/9849485/

[18] M. Moltafet, M. Leinonen, M. Codreanu, and R. D. Yates, "Status update control and analysis under two-way delay," *IEEE/ACM Trans. Networking*, vol. 31, no. 6, pp. 2918–2933, Dec. 2023. [Online]. Available: https://ieeexplore.ieee.org/document/10120660/

[19] G. Yao, C.-C. Wang, and N. B. Shroff, "Age minimization with energy and distortion constraints," in *Proc. 24th Int. Symp. Theory, Algor. Found., and Prot. Design for Mobile Netw. and Mobile Comput. (MobiHoc '23)*, ser. MobiHoc '23. Washington, DC, USA: Association for Computing Machinery, 2023, p. 101–110. [Online]. Available: https://doi.org/10.1145/3565287.3610266

[20] Y. Zou, K. T. Kim, X. Lin, and M. Chiang, "Minimizing age-of-information in heterogeneous multi-channel systems: A new partial-index approach," in *Proc. 22nd Int. Symp. Theory, Algor. Found., and Prot. Design for Mobile Netw. and Mobile Comput.* Shanghai China: ACM, Jul. 2021, pp. 11–20. [Online]. Available: https://dl.acm.org/doi/10.1145/3466772.3467030

[21] Y. Chen, J. Wang, X. Wang, and J. Song, "Age of information optimization in multi-channel network with sided information," *IEEE Commun. Lett.*, vol. 27, no. 3, pp. 1030–1034, Jun. 2023.

[22] G. Chen, Y. Chen, J. Wang, and J. Song, "Scheduling to minimize age of synchronization in multi-channel time-sensitive networks," in *2022 IEEE Wireless Commun. and Netw. Conf. (WCNC)*. Austin, TX, USA: IEEE, Apr. 2022, pp. 1605–1610. [Online]. Available: https://ieeexplore.ieee.org/document/9771855/

[23] E. Altman, R. El-Azouzi, D. S. Menasche, and Y. Xu, "Forever young: Aging control for smartphones in hybrid networks," in *Proc. 20th ACM Int. Symp. on Mobile Ad Hoc Netw. and Comput.*, 2019, pp. 91–100. [Online]. Available: http://arxiv.org/abs/1009.4733

[24] J. Pan, A. M. Bedewy, Y. Sun, and N. B. Shroff, "Age-optimal scheduling over hybrid channels," *IEEE Trans. Mobile Comput.*, vol. 22, no. 12, pp. 7027–7043, 2023.

[25] X. Song and J. Liu, "Performance of multiversion concurrency control algorithms in maintaining temporal consistency," in *Proc. 14th Annu. Int. Comput. Softw. and Appl. Conf.* Chicago, IL, USA: IEEE Comput. Soc. Press, 1990, pp. 132–139. [Online]. Available: http://ieeexplore.ieee.org/document/139341/

[26] S. Kaul, R. Yates, and M. Gruteser, "Real-time status: How often should one update?" in *2012 IEEE INFOCOM - IEEE Conf. Comput. Commun.* Orlando, FL, USA: IEEE, 2012, pp. 2731–2735. [Online]. Available: http://ieeexplore.ieee.org/document/6195689/

[27] D. P. Bertsekas, "Introduction to infinite horizon problems," in *Dynamic Programming and Optimal Control*, 4th ed. Belmont, MA: Athena Scientific, 2012, vol. 2, ch. 5 sec. 6, pp. 267–277.

[28] W. J. Lee and C.-C. Wang, "Aoi-optimal scheduling for arbitrary k-channel update-through-queue systems," in *Proc. IEEE Int. Symp. Inf. Theory (ISIT)*, 2024, p. 6. [Online]. Available: https://engineering.purdue.edu/~chihw/pub_pdf/24C_AoI_multi.pdf

[29] R. D. Yates, "Lazy is timely: Status updates by an energy harvesting source," in *2015 IEEE Intl. Symp. Inform. Theory (ISIT)*. Hong Kong, Hong Kong: IEEE, Jun. 2015, pp. 3008–3012. [Online]. Available: http://ieeexplore.ieee.org/document/7283009/

[30] A. Arafa, J. Yang, S. Ulukus, and H. V. Poor, "Age-minimal transmission for energy harvesting sensors with finite batteries: Online policies," *IEEE Trans. Inform. Theory*, vol. 66, no. 1, pp. 534–556, Jan. 2020. [Online]. Available: https://ieeexplore.ieee.org/document/8822722/

[31] A. Gosavi and V. K. Le, "Maintenance optimization in a digital twin for industry 4.0," *Ann. Oper. Res.*, pp. 1–25, 2022.

APPENDIX A
PROOF OF PROPOSITION 2

If the state $s = \Delta(t)$ satisfies $s < \beta^* - E(Y^{[k]})$, i.e., s is on the left-hand side of the vertex of the quadratic curve $Q_k^\circ(s, 0, \beta^*)$, see Fig. 4, then increase s value by a small $w > 0$ will lead to $Q_k^\circ(s + w, 0, \beta^*) = Q_k^\circ(s, w, \beta^*) < Q_k^\circ(s, 0, \beta^*)$, where the equality is by (13). By the same reasoning but going one step deeper, the best strategy under the starting state s is to set the waiting time $w^* = \beta^* - \mathbb{E}(Y^{[k]}) - s$ so that after waiting for w^* time the new $s' = s + w^*$ will "hit" the vertex, the lowest point of the quadratic curve $Q_k^\circ(s, 0, \beta^*)$.

On the other hand, if $s \geq \beta^* - \mathbb{E}(Y^{[k]})$, i.e., s is on the right-hand side of the vertex, we then set the waiting time $w^* = 0$ since we have already passed the vertex and any additional waiting time $w > 0$ will increase the cost: $Q_k^\circ(s + w, 0, \beta^*) = Q_k^\circ(s, w, \beta^*) > Q_k^\circ(s, 0, \beta^*)$.

If we plot $\min_{w \geq 0} Q_k^\circ(s, w, \beta^*)$ versus s, see Fig. 4, the new curve is a flat line on the left-hand side of the vertex but a quadratic curve on the right-hand side of vertex.

APPENDIX B
PROOF OF PROPOSITION 2 (CONVEX OPTIMIZATION VER.)

The optimization problem of Proposition 2 is as follows.

$$\begin{aligned} \min_{w} \quad & Q_k^\circ(s, w, \beta^*) \\ \text{s.t.} \quad & w \geq 0 \end{aligned} \tag{22}$$

Since $Q_k^\circ(s, w, \beta^*)$ is convex over s and the constraint w is a linear function, the optimization problem is a convex optimization problem. A Lagrangian of the optimization problem can be defined as

$$\mathcal{L}(w, \lambda) = Q_k^\circ(s, w, \beta^*) - \lambda w \tag{23}$$

A dual function is defined by

$$g(\lambda) \triangleq \inf_{w} \mathcal{L}(w, \lambda) \tag{24}$$

where dual problem is formulated as

$$\begin{aligned} \max_{\lambda} \quad & g(\lambda) \\ \text{s.t.} \quad & \lambda \geq 0 \end{aligned} \tag{25}$$

Given that

$$\frac{\partial}{\partial w}\mathcal{L}(w, \lambda) = \Big((s + w) - \Big(\beta^* - \mathbb{E}(Y^{[k]})\Big)\Big) - \lambda \tag{26}$$

It follows that

$$w^* = \max\Big(\Big(\beta^* - \mathbb{E}(Y^{[k]})\Big) - s + \lambda, 0\Big) \tag{27}$$

Thus, we have

$$g(\lambda) = \mathcal{L}(w^*, \lambda) \tag{28}$$

$$= \frac{\big((s + w^*) - \big(\beta^* - \mathbb{E}(Y^{[k]})\big)\big)^2}{2} + \mathcal{H}_k \tag{29}$$

$$= \begin{cases} -\frac{1}{2}\lambda^2 + (s - \theta_k)\,\lambda + \mathcal{H}_k & \lambda > s - \theta_k \\ \frac{1}{2}\,(s - \theta_k)^2 + \mathcal{H}_k & \lambda \leq s - \theta_k \end{cases} \tag{30}$$

where $\theta_k = \beta^* - \mathbb{E}(Y^{[k]})$. The solution λ^* such that satisfies $\frac{\partial g}{\partial \lambda}(\lambda^*) = 0$ is

$$\lambda^* = (s - \theta_k)^+ \tag{31}$$

Thus, the solution to the dual problem is

$$g(\lambda^*) = \begin{cases} \frac{1}{2}(s-\theta_k)^2 + \mathcal{H}_k & s > \theta_k \\ \mathcal{H}_k & s \le \theta_k \end{cases} \tag{32}$$

Since the Karush-Kuhn-Tucker (KKT) conditions are satisfied, strong duality holds. Therefore,

$$\begin{aligned} Q_k^\star(s, \beta^*) &= \min_{w \ge 0} Q_k^\circ(s, w, \beta^*) && (33)\\ &= g(\lambda^*) && (34)\\ &= \begin{cases} \frac{1}{2}(s-\theta_k)^2 + \mathcal{H}_k & s > \theta_k \\ \mathcal{H}_k & s \le \theta_k \end{cases} && (35) \end{aligned}$$

Therefore, due to the complementary slackness, the optimal waiting time w^* is given as

$$\begin{aligned} w^* &= \max(\beta^* - \mathbb{E}(Y^{[k]}) - s, 0) && (36)\\ &= \max\{w \ge 0 : w + s + \mathbb{E}(Y^{[k]}) \ge \beta^*\}. && (37) \end{aligned}$$

Appendix C
Proof Sketh of Lemma 1

We get a closed form of $f_\gamma(\mathbb{E}(Y^{[i]}), \mathbb{E}(Y^{[j]}), \mathcal{H}_i - \mathcal{H}_j)$ as below.

$$\begin{aligned} &f_\gamma(\mathbb{E}(Y^{[i]}), \mathbb{E}(Y^{[j]}), \mathcal{H}_i - \mathcal{H}_j) \\ &= \begin{cases} \gamma_A & \frac{(\mathbb{E}(Y^{[j]}) - \mathbb{E}(Y^{[i]}))^2}{2} < \mathcal{H}_i - \mathcal{H}_j \\ \gamma_B & \frac{(\mathbb{E}(Y^{[i]}) - \mathbb{E}(Y^{[j]}))^2}{2} \ge \mathcal{H}_i - \mathcal{H}_j \end{cases} \end{aligned} \tag{38}$$

where

$$\gamma_A = \frac{\mathcal{H}_i - \mathcal{H}_j}{\mathbb{E}(Y^{[i]}) - \mathbb{E}(Y^{[j]})} + 0.5(\mathbb{E}(Y^{[i]}) + \mathbb{E}(Y^{[j]})) \tag{39}$$

$$\gamma_B = \mathbb{E}(Y^{[j]}) - \sqrt{2(\mathcal{H}_i - \mathcal{H}_j)} \tag{40}$$

Proof. When $\mathcal{H}_i > \mathcal{H}_j$, we exactly have one intersection of $Q_i^\star(s, \beta^*)$ and $Q_j^\star(s, \beta^*)$. Let the intersection of two functions be (s^*, Q^*). Then , there are two cases: (i) $Q^* > \mathcal{H}_i$, which is equivalent to $\frac{(\mathbb{E}(Y^{[j]}) - \mathbb{E}(Y^{[i]}))^2}{2} < \mathcal{H}_i - \mathcal{H}_j$. In this case, the intersection lies on the right-hand side of both $Q_i^\star(s, \beta^*)$ and $Q_j^\star(s, \beta^*)$. Thus, by solving an equation of two quadratic functions, one can easily get $s^* = \beta^* - \gamma_A$. (ii) $Q^* = \mathcal{H}_i$, which is equivalent to $\frac{(\mathbb{E}(Y^{[j]}) - \mathbb{E}(Y^{[i]}))^2}{2} \ge \mathcal{H}_i - \mathcal{H}_j$. In this case, the intersection lies on the left-hand side of $Q_i^\star(s, \beta^*)$ and the right-hand side of $Q_i^\star(s, \beta^*)$. We can get $s^* = \beta^* - \gamma_B$ by calculating an equation of one quadratic function and one constant function. □

Appendix D
Proof Sektch of Lemma 2

By the transition probability discussion in (11), the (random) state $\tilde{s}$ that can be reached by any arbitrary action choice (k, w) and any arbitrary starting state s is less than $y_{\max} + \max_k \mathsf{Lag}_k$ with probability one. Therefore, the right-hand side of the Bellman equation only uses $h(\tilde{s})$ for those $\tilde{s} \in [0, y_{\max} + \max_k \mathsf{Lag}_k]$. As a result, any $h(s)$ with $s > y_{\max} + \max_k \mathsf{Lag}_k$ only appears in the left-hand-side of (11), which does not impose any "constraint" when solving the Bellman equation and can thus be ignored during numerical computation.

Appendix E
Proof sketch of the correctness of Algorithm 1

By the definition of j_0, for all $i > j_0$, we have $Q_i^\star(s, \beta^*) \ge Q_{j_0}^\star(s, \beta^*)$. Thus, line 8 $\gamma_k \leftarrow \infty$ for $k \in [j_0, K]$ is justifiable. Also by the definition of j_0, for all $i < j_0$, $Q_i^\star(s, \beta^*) \ge Q_{j_0}^\star(s, \beta^*)$ during the range of $s \le \beta^* - \mathbb{E}(Y^{[j_0]})$. For any (i, j) such that $\tilde{\gamma}_{i,j}$ is uniquely defined by Line 4, define $\theta_{i,j} = \beta^* - \tilde{\gamma}_{i,j}$. We now run the for a loop until and including Line 10 for the very first time and thus finished computing the $\tilde{\gamma_{i_0,j_0}}$ value for the very first time. For i_0 such that $i_0 = -\infty$, then we must have $Q_{i_0}^\star(s, \beta^*) \ge Q_{j_0}^\star(s, \beta^*)$ for all $i_0 < j_0$ during the range of $s > \beta^* - \mathbb{E}(Y^{[j_0]})$. Thus, if $i_0 = -\infty$, $Q_{j_0}^\star(s, \beta^*)$ is the lower envelope of $Q_{i_0}^\star(s, \beta^*)$ for all $i_0 \in \mathcal{C}$. Since the while loop stops in this case. Our algorithm is correct.

If $i_0 \ge 1$, then we must have $Q_{i_0}^\star(s, \beta^*) \ge Q_{j_0}^\star(s, \beta^*)$ during the range of $s \in (\beta^* - \mathbb{E}(Y^{[j_0]}), \theta_{i_0,j_0}^+]$. Here θ_{i_0,j_0}^+ indicates a value $\theta_{i_0,j_0} + \delta$ for some sufficiently small but strictly positive $\delta > 0$. Furthermore, $Q_{i_0}^\star(s, \beta^*)$ is the lower envelope during the range $s \in [\theta_{i_0,j_0}, \theta_{i_0,j_0}^+]$. The above discussion shows that for the very first (i_0, j_0), we have characterized the lower-envelop for the range of $s \le \theta_{i_0,j_0}^+$ after finishing Line 12 of the while loop. We now use mathematical induction.

Hypothesis: Suppose we have successfully characterized the lower envelop for the range of $s \le \theta_{i_0,j_0}^+$ for some pair of (i_0, j_0), not necessarily the first one. Also, assume that $Q_{i_0}^\star(s, \beta^*)$ is the lower[5] envelope during the range $s \in [\theta_{i_0,j_0}, \theta_{i_0,j_0}^+]$ for that particular (i_0, j_0), not necessarily the first pair. We now like to prove that *after one iteration of the while loop, the induction hypothesis still holds with the new* $(\tilde{i}_0, \tilde{j}_0)$.

Induction: If $i_0 = 1$, the while loop stops in the next iteration since $\tilde{j}_0 = i_0 = 1$. Because no further γ_k is assigned, our algorithm assumes the lower envelope will extend from θ_{i_0,j_0}^+ to ∞. This assumption turns out to be correct since $Q_1^\star(s, \beta^*)$ is the lower envelop during $[\theta_{1,j_0}, \theta_{1,j_0}^+]$ implies that it is also the envelope during $[\theta_{1,j_0}, \infty)$

If $i_0 \ge 2$, then we have $\tilde{j}_0 = i_0 \ge 2$. Consider two cases: **Case 1:** If $\tilde{i}_0 = -\infty$ and $\theta_{\tilde{j}_0,i}$ exists for some $i > \tilde{j}_0 = i_0$, then $\theta_{\tilde{j}_0,i} \le \theta_{i_0,j_0}$. Suppose there exists an $i' > i_0$ such that $\theta_{i_0,i'} > \theta_{i_0,j_0}$. This contradicts that $Q_{i_0}^\star(s, \beta^*)$ is the lower

[5]If two curves overlap, the lower envelope is defined as the unique one with the smallest channel index. Therefore, there is no tie in our definition.

envelope in the range of $s \in [\theta_{i_0,j_0}, \theta^+_{i_0,j_0}]$. Thus, in the case of $\tilde{i}_0 = -\infty$, the curve $Q^\star_{i_0}(s, \beta^*)$ is also the lower envelope in the range of $s \in [\theta_{i_0,j_0}, \infty)$. Since Algorithm 1 stops in this case, it correctly characterizes the entire lower envelope again.
Case 2: $\tilde{i}_0 \geq 1$. If $\tilde{i}_0 \geq 1$, then $\theta_{\tilde{i}_0,\tilde{j}_0} > \theta_{i_0,j_0}$. Suppose there exists an $i' < i_0$ such that $\theta_{i',i_0} \leq \theta_{i_0,j_0}$. This contradicts that $Q^\star_{i_0}(s, \beta^*)$ is the lower envelope in the range of $s \in [\theta_{i_0,j_0}, \theta^+_{i_0,j_0}]$. Also, I claim if $\tilde{i}_0 \geq 1$ and $\theta_{\tilde{j}_0,i}$ exists for some $i > \tilde{j}_0 = i_0$, then $\theta_{\tilde{j}_0,i} \leq \theta_{i_0,j_0}$. Suppose there exists an $i' > i_0$ such that $\theta_{i_0,i'} > \theta_{i_0,j_0}$. This contradicts that $Q^\star_{i_0}(s, \beta^*)$ is the lower envelope in the range of $s \in [\theta_{i_0,j_0}, \theta^+_{i_0,j_0}]$. Therefore, we have that if $\tilde{i}_0 \geq 1$, then $Q^\star_{i_0}(s, \beta^*)$ is the lower envelope in the range of $s \in [\theta_{i_0,j_0}, \theta_{\tilde{i}_0,\tilde{j}_0}]$ and $Q^\star_{\tilde{i}_0}(s, \beta^*)$ is the lower envelope in the range of $s \in [\theta_{\tilde{i}_0,\tilde{j}_0}, \theta^+_{\tilde{i}_0,\tilde{j}_0}]$. By induction, the proof is complete.